New laboratory core flooding experimental system for EOR surfactant screening, especially for foam

Xuesong Li[1,*], and *Matthias* Appel[1]

[1]Shell Global Solutions International B.V., Special Core Analysis Team, 1031HW Amsterdam, The Netherlands

Abstract. Core flooding experiments are often used to assess the performance of EOR techniques or to screen surfactants. An inherent success factor of chemical EOR processes is the choice of the optimal surfactant which is a trade-off between process performance and economic considerations. Currently, this trade-off can often not fully be evaluated with laboratory experiments because the associated experiments are time consuming which typically limits their number and, in turn, impacts the reliability of the results. For this reason, we aimed to develop an automated and parallel core flooding unit to conduct faster, cheaper and reliable tests for EOR technologies. The benefit of doing this is to dramatically increase the statistics of EOR-related experimentation while decreasing the manpower needed, leading to a much better value-to-cost ratio. As a first step, we designed a setup which is applicable for multiple EOR-related core flooding experiments, such as alkaline-surfactant polymer (ASP), low salinity, polymer flooding or foam injection. The device can be used for co- or sequential injection of gas, water and oil. For the high compressibility gas phase, it is often desirable to regulate its in-core volumetric flow rate. We control the gas flow using inline sensors and flow meters corresponding to the real time in situ core pressure. With a feedback loop, the offset of gas flow can be automatically updated within 0.1% deviation from the target setting. By miniaturizing the core sample and simplifying the experimental procedures, the automated flooding process achieved 90% efficiency gain while reducing sample consumption. This proof of concept can easily be further evolved into a parallelized system. Experience with this new core flooding system demonstrated the dramatic increase in screening capacity and added value to the EOR development workflows.

1 Introduction

There is general consensus about an increasing energy demand in the coming decades. Irrespective of the fact that renewable energy will play an increasing role in the energy supply, the contribution of oil for energy consumption and as feed for chemical production will remain high and is expected to grow. [1]. The current oil market requires a relatively low recovery cost for any field development [2-4] which, in turn, requires faster technology deployment and adequate evaluation of the associated technical risks.

In typical hydrocarbon recovery scenarios, after a primary and secondary recovery, there is still a larger percentage of oil (30-60%) remaining in the reservoir. This remaining oil is primarily trapped by capillary forces [5]. Enhanced oil recovery (EOR) techniques often utilize surfactants to either reduce the interfacial tension between the aqueous phase and oil phase or generate foam to increase the swept efficiency of gas injection [6]. In any of these processes, the selection of the surfactant is essential for the incremental oil recovery. From an economical point of view the cost of surfactant is also a substantial element of the cost of EOR projects [7, 8]. However, the surfactant performance depends on the reservoir fluid and rock properties at field-related temperature and pressure conditions Therefore, it would be ideal to conduct core flooding experiments which combine all these factors for surfactant selections. But when taking all the influencing parameters into account the screening matrix can be very large. For example, Table 1 illustrates the screening program for foam surfactant screening [9]. Even this fairly slimmed down screening program has a matrix size of 100, which would take a few years to complete using a conventional core flooding setup.

Table 1. EOR surfactant screening matrix with reduced variation of variables.

Variables		Variations
1	rock sample type	1
2	rock permeability	1
3	brine salinity	1
4	crude oil	1
5	surfactant type	5
6	surfactant concentration	2
7	rock sample dimension	1
8	flow rate	2
9	temperature	1
10	pressure	1
11	gas/liquid ratio in one test	5
combinations/test numbers		100

* Corresponding author: xuesong.x.li@shell.com

Conventional core flooding approaches can often take up to a month (often more than a week) to complete a single core flooding experiment and are not sufficient for the screening target [9, 10]. Keeping this in mind, a new high throughput core flooding unit was developed for the selection of EOR surfactants or related chemicals. A similar effort was published by Baldygin et al.. Their system comprised sand pack samples in combination with liquid flooding [11].

The efficiency gains of the new system presented in this study is a result of three main improvements compared to a conventional core flooding design. Firstly, a smaller core sample with a reduced diameter is used which minimizes the sample rock and fluid consumptions and responds faster to fluid injections. For this reason our new core flooding setup using a minimized rock sample was named "Lilliput" [12], which will be referred to in the following sections as the new core flooding system discussed in this paper. Secondly, in-line sensors and flow meters are used for flow control, and, together with an integrated computer program, a feedback loop enables an automatic core flooding process. Lastly, the whole setup is designed with simplified operation procedures, such as the use of an oven with a sliding base that allows for easy access to all components of the system. The high-pressure fluid vessels and core holders are designed with finger-tight nuts that simplify assembly as well as a "plug and play" design of the core sample installation. As a consequence, the Lilliput core flooding system is at least 10 times more efficient than the conventional core flooding unit in terms of required experimental duration as 2 weeks of conventional core flooding are reduced to a single-day experiment.

2 Detailed Design

2.1 Flow diagram

The Lilliput core flooding unit consist of three main parts: the fluid injections and controls, the core holder unit where fluid floods through the rock sample and the outflow of the core flooding unit including the effluent analysis and back pressure regulation. A flow diagram of the Lilliput unit is shown in Fig. 1.

Two Quizix™ pumps (QX6000 series, with 410 bar working pressure, flow rate ranging from 0.001mL/min to 50 mL/min, cylinder volume 12.3 mL) are utilized to deliver the sample fluid. One pump is connected to three parallel high-pressure vessels used as the reservoir for the aqueous phase; another pump is connected to the oil reservoir. The gas phase, either N_2 or CO_2 from gas cylinders is connected to the inlet of the core with the gas flow rate regulated by a Bronkhorst™ gas flow meter (EL-flow series, working pressure of 100 bar). Depending on the screening purposes, the injection fluid can be switched sequentially between the aqueous phase, the oil phase or gaseous phase, with two phases co-injection or three phases joint injections.

The high-pressure fluid vessels (manufactured in-house with a design pressure of 200 bar, temperature 200°C) are placed together with a core holder in an oven. Prior to any fluid injection, the fluids and rock sample are heated up to the target experimental temperature. To minimize the risk of corrosion, all the wetting parts in the oven are made of HC276™. Due to the smaller core sample and thus smaller pore volumes, the capacity of the 4 fluid vessels is sufficient to provide continued core flooding for 400 pore volumes (PV).

The fluid that comes out of the core will first pass through a cooler and then through an in-line Bronkhorst liquid mass flow meter (mini CORI-FLOW™ Coriolis) for the effluent oil fraction analysis. This meter is applicable for the liquid phase, e.g. oil and brine, or emulsion phase mass flowrate measurement A membrane type back pressure regulator is connected before the fluid is vented from the system. The maximum temperature of the setup is 120°C and the maximum operating pressure is 100 bar.

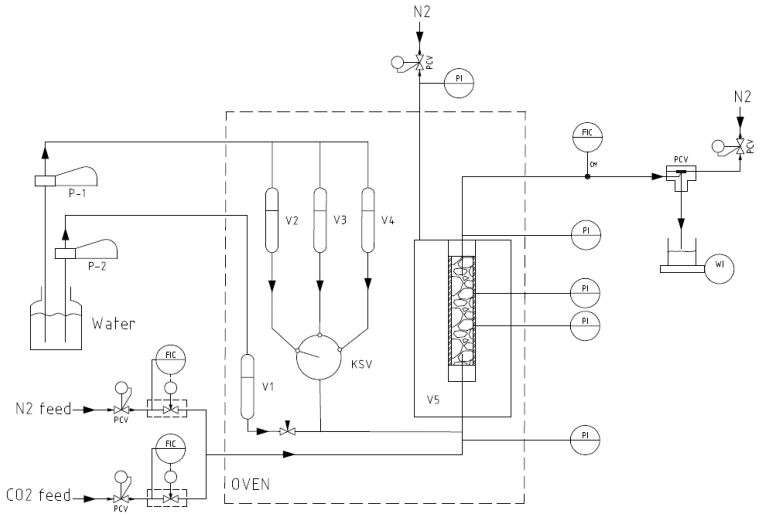

Fig. 1. Flow diagram of the core flooding for general EOR screening. P-1 and P-2: Quizix pump; V1, V2, V3, V4: High pressure fluid vessel with piston; KSV: switch valve; PCV: pressure control valve; FIC: flow indicator/controller; PI: pressure transducer; WI: weight indicator.

2.2 Core holder

The core holder is an important element of a core flooding unit. In conventional core flooding setup, there are a few typical sizes for the core, from 1 inch to 3 inches in diameter, and with a length from 5 cm to 1 m. The core samples used on Lilliput setup have a smaller diameter, 1 cm, and a variable length between 5 cm to 17 cm. The choices of core sample length depend on the available material and the purpose of the experiment. For less consolidated rock, long and slim core samples are fragile and difficult to prepare. In such cases, the rock samples are used together with two end dummy pieces made from PEEK with a 1mm inner diameter fluid pass to make up the total length of 17 cm. Due to the choice of a smaller diameter the total pore volume is significantly reduced. As a result, it takes less time to reach a steady flooding state under the same flooding condition compared to a larger core.

The core holder is placed vertically, and the flooding direction is from the bottom to the top. During a core flooding experiment the cylindrical surfaces need to be sealed to prevent fluid stream flow at the surface of the core. Often epoxy sealing or confining pressure on rubber sleeves are used in conventional core flooding setup [13, 14]. In the Lilliput unit, the "plug and play" core assemble is realized by using rubber sleeves to seal the cylindrical surface, see Fig. 2. While loading or unloading a rock sample to the core holder, vacuum pressure is applied outside of the rubber sleeve to enlarge the diameters of the sleeve. During the fluid flooding stage, confining pressure is applied outside of the sleeve with a pressure approximately 10 bar higher than the highest fluid pressure in the core. Two high pressure metal tips connected to the pressure transducers with distance of 5 cm are fixed to the rubber sleeve body. These tips are designed to avoid direct contact with the rock sample, which prevents any damage from occurring during the rock sample installation. The two pressure tips endure expansion or restriction of the rubber sleeve around the tips during the experiment. The core sleeve withstands the required 90 bar pressure difference [15], demonstrating a good sealing performance and functioning as the key time saver during the core assembling process.

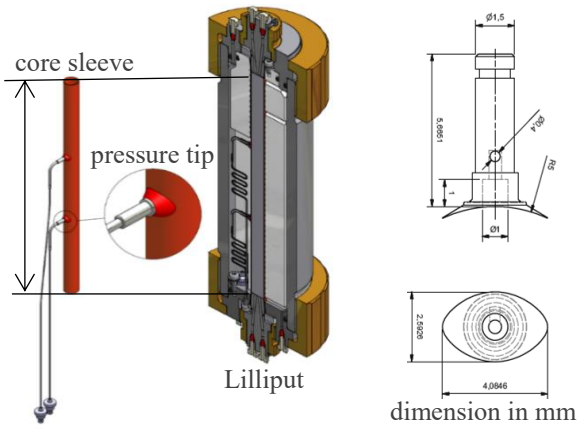

Fig. 2. Core holder design using rubber sleeve with moulded in mini pressure tip.

With this design of the rubber sleeve, the core installation or unloading time takes only 5 minutes, instead of typically several hours for a conventional Hassler-type core holder using sleeves, or even days if one chooses to use epoxy which involves epoxy aging, side pressure tip drilling and excess epoxy trimming. In the Lilliput unit the core changing procedure only involves opening the oven, turning the hand-tight-nuts and switching the confining pressure to vacuum, see Fig. 3. The core mounting process is dramatically simplified.

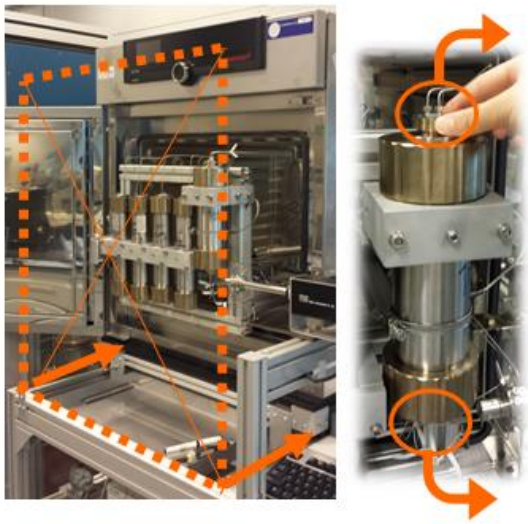

Fig. 3. Instruction of core holder installation on Lilliput setup with sliding oven and hand-tight nut.

2.3 Feedback loop control

During the core flooding experiment, the automated flooding process is regulated by a feedback loop control program, as show in Fig. 4. Depending on the purpose of the experiment, different criteria are chosen for controlling the core flooding program. First, the flooding fluids are pumped into the core with an initial flow rate given by the operator. Once the flow has started, the sensors around the core measure temperature, pressures, flowrate and effluent composition. These measurements are acquired by the computer program every 5 seconds. By reading these inputs, the computer program judges the in-situ flow status and regulates the fluid flow accordingly.

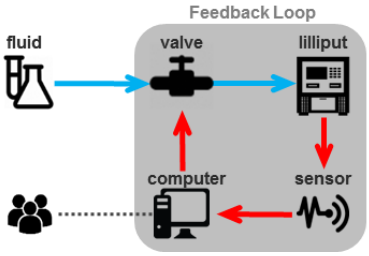

Fig. 4. Computer controlled feedback flow regulation on Lilliput core flooding unit.

The main benefit for the feedback loop control is enabling an automatic flooding process with limited

* Corresponding author: xuesong.x.li@shell.com

human supervision. Some of the conventional core flooding units can run through the flooding program with user-defined flooding steps. But often these approaches suffer from either long running periods for each step to ensure a steady state is reached or it requires constant monitoring by the operator.

Gases are often injected into oil reservoirs to enhance oil recovery. Due to the much lower gas viscosity compared to reservoir liquid phases, gas can have early break-through to the production well or might be fingering to the top of the reservoir without efficiently displacing the oil. Foam can achieve better conformance control. One of the important parameters used to quantify the effect of foam is by identifying the extra flow resistance created by foam.

Taking a foam resistance factor experiment as example, it would be ideal to have a constant total volumetric flow rate in the core for the performance evaluation [16]. However, due to the high gas compressibility, the manual regulation of gas flow is challenging and often introduces several percent, sometimes even 20%, uncertainty [17]. The computer-regulated foam flooding experiment is efficient and more precise as shown in Fig. 5, where the automatic fluid flow regulation by the computer program and the result of the experiment are presented. During the whole period, from 2400 s to 6500 s, there was no user-interference by the operator. All steps are completed by the computer automatically.

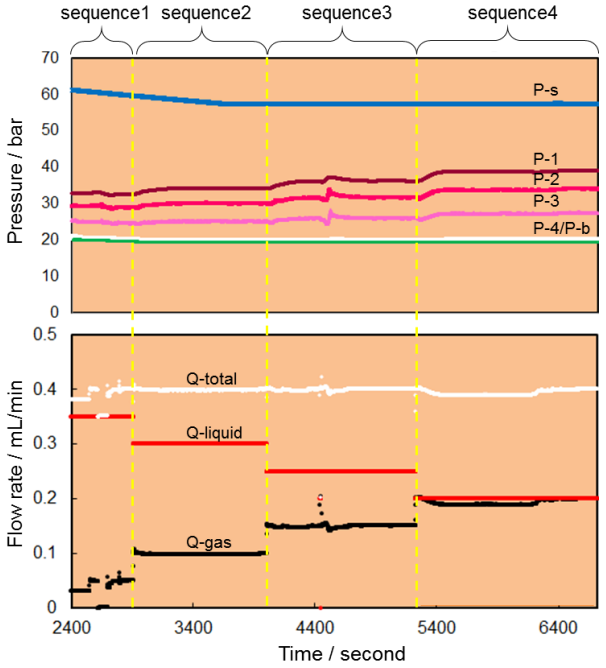

Fig. 5. Automatic core flooding processes for a foam resistance factor experiment. The four user-predefined flooding sequences have different foam gas/liquid ratios. The switch between sequences are done by the computer program by judging flow status criteria, here pressure stability. P-s: core sleeve confining pressure; P1, P2, P3, P4: 4 pressures point distributed along the core with the same distances; P-b: back pressure. Q-total, liquid, gas: in situ volumetric flow rate in total, for liquid and for gas, automatically regulated by the feedback flow control programme, using equation (9) below

The user input to the computer are 4 flowing sequences with constant total in-situ volumetric flow rates and changing the gas/liquid ratio. Instead of specifying the flooding, the target criteria that the program uses is that of steady flow; e.g., the stabilization criterium of the steady pressure gradient can be given as input. The four different steps are taking different times to complete, and at the end of each step both the target total in-situ volumetric is regulated within 0.5% offset and a stable flooding state are reached. The average flooding time for completing one sequence is only around 16 minutes.

A mobility reduction factor (MRF) number is often the required parameter derived from foam core flooding experiments. It is the apparent viscosity ratio of foam and gas flooding. Referring to Darcy's law, the apparent viscosity of the fluid in the core can be expressed as below,

$$Q_{v-core} = \frac{\pi R^2 \cdot K_{liquid} \cdot \Delta p}{\mu L} \tag{1}$$

$$\frac{\pi R^2 \cdot K_{liquid}}{L} = constant = \mathrm{C} \tag{2}$$

$$\frac{Q_{v-core} \cdot \mu}{\Delta p} = \mathrm{C} \tag{3}$$

$$\mu = \frac{\mathrm{C} \cdot \Delta p}{Q_{v-core}} \tag{4}$$

where, R is the radius of the core, Δp is the pressure drop over the core, and L is the length of the core, K_{liquid} is the permeability of the liquid in the core, Qv is the volumetric flow rate, and μ is the apparent viscosity, since foam is compressible, so for the same amount of gas the volume of it are different in the line and in the core. The ratio of $Q_{\mathrm{v\text{-}core}}$ and $Q_{\mathrm{v\text{-}line}}$ can be written as,

$$\frac{Q_{v-core}}{Q_{v-line}} = \frac{V_{gas-core} + V_{water-core}}{V_{gas-line} + V_{water-line}} \tag{5}$$

where V is the volume of the fluid, with known gas fraction, *fg-line* in the line. For N_2 the dependency of density on pressure at the same temperature condition is nearly linear, written as below,

$$\frac{V_{gas-line}}{V_{gas-core}} = \frac{\rho_{gas-core}}{\rho_{gas-line}} = \frac{a \cdot p_{core} + b}{a \cdot p_{line} + b} \tag{6}$$

where a, b are the known parameter of the linear relationship shown in Fig. 6 [18], and ρ is the density. For a simple model below, with p_0 as the gas pressure in the line before entering the core, and p_1, p_2 as the pressure at the inlet and outlet of the core. The apparent viscosity can be written further as equation (7),

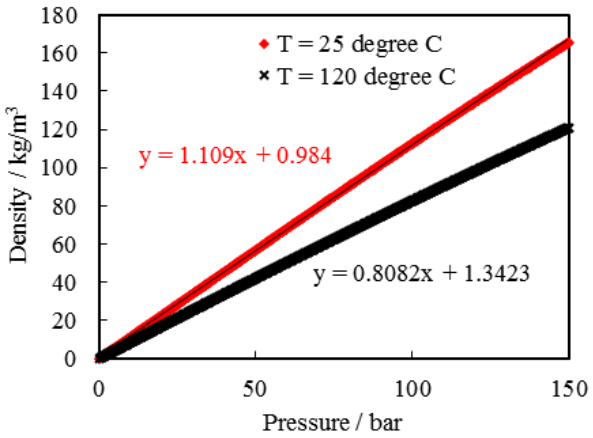

Fig. 6. The dependency of N_2 density on pressure at different temperatures.

$$\mu = \frac{C}{Q_{v-line}} \cdot \frac{p_1 - p_2}{\left[\frac{ap_0 + b}{a\left(\frac{p_1 + p_2}{2}\right) + b} - 1\right] \cdot f_{g-line} + 1} \tag{7}$$

Using conventional core flooding units, the apparent viscosity is calculated by equation (7) using the controlled gas volume in the line. For the Lilliput unit, $Q_{v\text{-core}}$ is automatically regulated to the target value. Here it is assumed that the pressure gradient in the core is constant and the in-situ core pressure can be represented by the average of p_1 and p_2. The gas fraction in line and in core has the relationship below,

$$k = \frac{ap_0 + b}{a\left(\frac{p_1 + p_2}{2}\right) + b} \tag{8}$$

$$\frac{f_{g-core}}{1 - f_{g-core}} = k \cdot \frac{f_{g-line}}{1 - f_{g-line}} \tag{9}$$

equation (9) is embedded in the computer program on Lilliput to control the in-situ gas fraction. It is a function of parameters including user defined $Q_{v\text{-core}}$, temperature. p_1 and p_2. It should be noticed that the nearly linear density dependency on pressure is only applicable to N_2, under the applicable working conditions. For CO_2, a non-linear approximation, together with the additional correction on the gas solubility in the fluid is applied.

With the above simplified core assembling procedure and the computer-controlled feedback loop, the time required for core flooding experiments using the Lilliput unit is compared with conventional larger core flooding experiments, see Table 2. In general, the efficiency gain is above 90% and the manpower requirement is dramatically reduced. In EOR surfactants or chemicals screening workflow, the rock and fluid samples are also prepared in batch to save time.

Table 2. Comparation of time consumption for delivering one core flooding experiment on average conventional medium size core flooding unit and on Lilliput unit.

Procedures	conventional (Φ: 2inches, L: 30 cm)	Lilliput (Φ: 1 cm, L: 17 cm)
1.Fluid sample filling to the reservoirs	10 minutes, for 20 PV flooding	10 minutes, for 400 PV flooding
2.Core sample mounting	8 hours for sleeve-seal; 2 days for epoxy-seal	5 minutes
3.User defined flooding sequences and criteria	5 minutes	5 minutes
4.Execution of the flooding, foam flooding at 20 feet/day	> 2 days machine time, (50% of time needs operator's supervision)	< 4 hour, (no supervision of the operator)
Total time	3 – 5 days	< 0.5 days

Notations: Φ: diameter; L: length; PV: pore volume

3 Screening performance evaluation

One of the concerns with using smaller core sample is the reliability of the result, especially for those screening cases aiming to provide the highest oil recovery recipes. In principle, the smaller the sample is, the more challenging it is to measure the oil production precisely. To compensate this drawback on the setup, both an inline density meter and mass balance are used to improve the accuracy for the effluent analysis. At the same time, the system has a compact design with a shortened flowline and reduced inner diameter of tubing to minimize the dead volumes. The dead volume before the core account for about 2.5% of an average pore volume of core sample, after the core, the dead volume is 5% of the pore volume

To validate the screening reliability of the Lilliput core flooding unit, two core flooding experiments also conducted on conventional core flooding units – experiments A and B - were reproduced on the Lilliput setup. The conventional core flooding unit has a before and after core dead volume about 5% and 6%, respectively, of average pore volume.

The experimental details of these two experiments are listed in Table 3. The purpose of ASP core flooding experiments discussed here is to quantify the performance of different ASP recipes regarding their EOR protentional. In brief, significant additional oil recovery from the ASP flooding was seen in a successful ASP formula design in experiment A but not experiment B for both setups.

Table 3. Details of the two reference experiments

Experiment A – high oil recovery	
Rock type	Berea
Core direction	vertical
Pore volume (mL)	122
Brine permeability at reservoir temp (mD)	74
Crude oil viscosity (mPa.s)	3.9

Brine viscosity at 80 °C (mPa.s)	0.4
Viscosity of ASP at 80 °C (mPa.s)	8.5
Pore volumes ASP injected (PV)	0.4
Pore volumes polymer injected (PV)	3
Viscosity of polymer at 80 °C (mPa.s)	8.6
Saturations:	
Original oil in place (OOIP) (mL)	67.5 ±6
Oil produced waterflood (%PV):	17±6
Oil produced ASP/Polymer flood(%PV):	34±6

Experiment B – low oil recovery	
Rock type	Berea
Core direction	vertical
Pore volume (mL)	121
Brine permeability at reservoir temp (mD)	75
Crude oil viscosity (mPa.s)	0.9
Brine Viscosity at T-reservoir (mPa.s)	0.4
Viscosity of ASP at 90 °C (mPa.s)	10.7
Pore volumes ASP injected (PV)	0.4
Pore volumes polymer injected (PV)	3
Viscosity of polymer at 90 °C (mPa.s)	7.3
Saturations:	
Original oil in place (OOIP) (mL)	75 ±6
Oil produced waterflood (%PV):	19±6
Oil produced ASP/Polymer flood(%PV):	6.6±6

The rock samples used for the evaluation are sandstone Berea outcrop rock with porosities of approximately 25% and permeabilities of approximately 100 millidarcy (mD). These rock samples are originally water-wet, and no pre-experiment treatment such as cleaning or aging with oil was applied to ensure consistency with the reference experiments. From an independent ASP core flooding experiment with CT-based saturation monitoring [19], no obvious capillary end effect was observed from 27 cm long cores, and capillary end effect is occurring within the 2 cm zone from 15 cm cores. In this study, the refence experiments use 30 cm long core samples, for which no significant capillary end effects during the water flood is expected. Furthermore, for the Lilliput setup, the core samples have a very slim and long shape (1cm in dimeter and 17 cm in length), where the capillary end effect is considered to have limited volumetric influence over the total pore volume. The capillary end effect correction can be made with the reference method [20], but within a screening focus in the work flow, this step was omitted. Identical oil saturation and brine flooding procedures are applied to the experiment on the Lilliput system and the reference study. In all steps, the same fluid and flooding speed was applied to both experiments. Different from the reference case, the flooding procedure on the Lilliput setup does not have an additional polymer drive after the ASP flooding, instead a slightly larger amount of 2-3 pore volumes of only ASP was injected to the core continually, with a subsequent brine drive as detailed in Table 4.

Table 4. Flooding procedures followed on the Lilliput setup and for reference experiment A

Steps	Flooding speed (feet/day)	Injection volume (PV)
brine permeability	60, 30, 20	around 30
Oil saturation	10	Around 15
Brine flooding	3	until no additional oil recovery
ASP flooding	3	2 to 3
Brine driving	3	5

For the re-executed experiment A, the additional oil production from ASP flooding is 1.9 mL. The additional oil recovery over the total pore volume is around 47%, see more detailed comparation are listed in Table 5,

Table 5. Comparing the experiment carried out on the Lilliput system with the reference experiment A

Items	Ref exp A	Lilliput
Rock permeability (mD)	74	105
Apparent ASP viscosity (cp)	16	13 - 18
Core dimension, Length/Diameter (cm)	30/5	17/1
ASP injection (PV)	0.4	3
Additional oil recovery % to the total PV	34 ± 6	47 ± 5

The pressure drop across the core during different flooding phases is another key parameter to identify the flooding behavior on the Lilliput setup. Figure 7 illustrates the apparent viscosity at the later stage of the ASP flooding period using the Lilliput system. This viscosity varies between 13 cp and 18 cp during the experiment, which is comparable to the value of the reference experiment (16 cp).

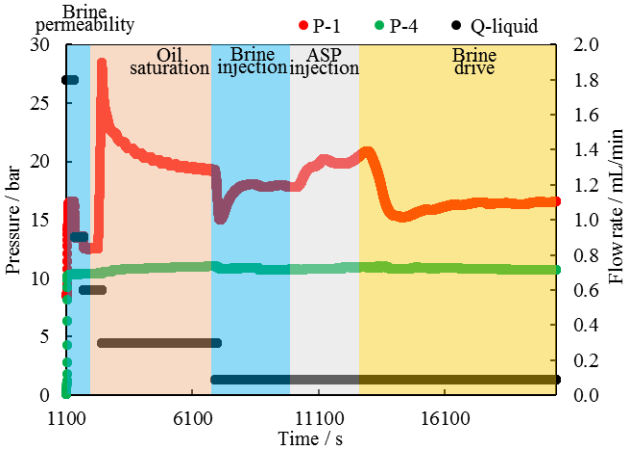

Fig. 7. Core flooding experiment on Lilliput unit. Four flooding periods: step 1, brine permeability measurement at three different injection rates; step 2, oil saturation period; step 3, ASP injecting period; step 4, brine drive. Steps are highlighted with different colour.

For experiment B, which was also reproduced on the Lilliput unit, the additional oil production from ASP solution flooding is approximately 0.3 mL. The additional oil recovery referenced to the total pore volume is approximately 10%, compared to the reference recovery

of 6.6%. For both the conventional and the Lilliput experiment, continually increasing apparent viscosities were observed during the ASP injection. The apparent viscosities after injecting 0.4 PV of ASP solution are 80 cp and 130 cp, respectively, for the reference- and the Lilliput experiments. For the experiment with the Lilliput system, the higher length-to-diameter ratio aggravated the injectivity issue, where a higher apparent viscosity was observed.

Table 6. Comparing the experiment carried out on Lilliput with the reference experiment B

Items	Ref exp B	Lilliput
Rock permeability (mD)	75	100
Apparent ASP viscosity (cp) 0.4 PV injection	80	130
Core dimension, Length/Diameter (cm)	30/5	17/1
Length/Diameter ratio	6	17
ASP injection (PV)	0.4	3
Additional oil recovery % to the total PV	6.6 ± 6	10 ± 5

For both cases tested, the additional oil recovery determined using the Lilliput system is in good agreement with the reference experiments, but both Lilliput results are also slightly higher than the reference experiments. This could be the result of the extra 2-3 pore volume of ASP solution injected during the experiments with the Lilliput system instead of 0.4 pore volume ASP plus polymer injected during the experiment with the conventional core flooding system. Even so, qualitatively the results obtained with the Lilliput systems demonstrate that this automated core flooding system can distinguish the efficiency of ASP solutions. This capability is typically sufficient for screening purposes of chemical EOR flooding.

Regarding efficiency, each core flooding experiment is completed within 1 day (24 hours) with the sample preparation done during the day and the automatic flooding taking place during the night. The experimental results are in good agreement with the references regarding the pressure gradient/apparent viscosity across the core and the fraction of additional oil recovery. The measurement of initial oil saturation and residual oil saturation measurement, which requires real time X-ray scanning are omitted during the evaluation. The estimation of additional oil recovery is simply based on the volume of oil produced during the ASP flooding phases.

4 Summary

The newly designed automated core flooding using smaller core samples and a fully automated experimental control and data acquisition system has demonstrated more than 90% efficiency gain compared to conventional core flooding systems, with dramatically streamlined operation and improved control of the gas flow regulation. For foam experiments, the unit demonstrated its high precision in in-situ flow control and in-situ gas/liquid ratio. The ASP experiment carried out with the Lilliput setup verified the reliability of replacing a larger core sample by a mini core. The “plug and play” core holder design, the simplified operational procedures, the automation feedback control loop and the utilization of smart sensors can be applied to conventional core flood setups to improve the efficiency. Parallel core flooding units with the same unit design can be used to boost the screening capacity further.

The project was carried out within Shell Global Solutions International B.V. During the development of this new core flooding unit, the workshop department was heavily involved and contributed to the designing and construction of the setup.

Reference

1. F. Fuso Nerini, J. Tomei, L. S. To, I. Bisaga, P. Parikh, M. Black*, et al.*, "Mapping synergies and trade-offs between energy and the Sustainable Development Goals," *Nature Energy,* vol. 3, pp. 10-15, 2018.
2. H. Guo, J. Dong, Z. Wang, H. Liu, R. Ma, D. Kong*, et al.*, "2018 EOR Survey in China-Part 1," presented at the SPE Improved Oil Recovery Conference, Tulsa, Oklahoma, USA, 2018.
3. B. Mukherjee, P. D. Patil, M. Gao, W. Miao, S. Potisek, and P. Rozowski, "Laboratory Evaluation of Novel Surfactant for Foam Assisted Steam EOR Method to Improve Conformance Control for Field Applications," presented at the SPE Improved Oil Recovery Conference, Tulsa, Oklahoma, USA, 2018.
4. S. Pal, M. Mushtaq, F. Banat, and A. M. Al Sumaiti, "Review of surfactant-assisted chemical enhanced oil recovery for carbonate reservoirs: challenges and future perspectives," *Petroleum Science,* vol. 15, pp. 77-102, 2018.
5. J. Chung, B. W. Boudouris, and E. I. Franses, "Surface tension behavior of aqueous solutions of a propoxylated surfactant and interfacial tension behavior against a crude oil," *Colloids and Surfaces A: Physicochemical and Engineering Aspects,* vol. 537, pp. 163-172, 2018.
6. A. B. Fuseni, A. M. AlSofi, A. H. AlJulaih, and A. A. AlAseeri, "Development and evaluation of foam-based conformance control for a high-salinity and high-temperature carbonate," *Journal of Petroleum Exploration and Production Technology,* pp. 1-8, 2018.
7. M. S. Kamal, A. Sultan, I. Hussein, S. Hussain, and A. M. AlSofi, "Screening of Surfactants and Polymers for High Temperature High Salinity Carbonate Reservoirs," in *SPE Kingdom of Saudi Arabia Annual Technical Symposium and Exhibition*, 2018.
8. N. Khazali, M. Sharifi, and M. A. Ahmadi, "Application of fuzzy decision tree in EOR screening assessment," *Journal of Petroleum Science and Engineering,* vol. 177, pp. 167-180, 2019.

9. P. Dong, M. Puerto, G. Jian, K. Ma, K. Mateen, G. Ren*, et al.*, "Exploring Low-IFT Foam EOR in Fractured Carbonates: Success and Particular Challenges of Sub-10-mD Limestone," in *SPE Annual Technical Conference and Exhibition*, 2018.
10. B. Wei, J. Ning, J. Shang, and W. Pu, "An experimental validation of a smart emulsion flooding for economic chemical EOR," in *SPE EOR Conference at Oil and Gas West Asia*, 2018.
11. A. Baldygin, D. S. Nobes, and S. K. Mitra, "New Laboratory Core Flooding Experimental System," *Industrial & Engineering Chemistry Research,* vol. 53, pp. 13497-13505, 2014.
12. J. Swift, "Gulliver's travels," in *Gulliver's Travels*, ed: Springer, 1995, pp. 27-266.
13. C. S. Gregersen, M. Kazempour, and V. Alvarado, "ASP design for the Minnelusa formation under low-salinity conditions: Impacts of anhydrite on ASP performance," *Fuel,* vol. 105, pp. 368-382, 2013.
14. M. M. Kulkarni and D. N. Rao, "Experimental investigation of miscible and immiscible Water-Alternating-Gas (WAG) process performance," *Journal of Petroleum Science and Engineering,* vol. 48, pp. 1-20, 2005.
15. S.-H. Chang and R. B. Grigg, "Laboratory Flow Tests Used To Determine Reservoir Simulator Foam Parameters for EVGSAU CO2 Foam Pilot," presented at the Permian Basin Oil and Gas Recovery Conference, 1994.
16. S. A. Jones, V. van der Bent, R. Farajzadeh, W. R. Rossen, and S. Vincent-Bonnieu, "Surfactant screening for foam EOR: Correlation between bulk and core-flood experiments," *Colloids and Surfaces A: Physicochemical and Engineering Aspects,* vol. 500, pp. 166-176, 2016.
17. R. D. Wyckoff and H. G. Botset, "The Flow of Gas-Liquid Mixtures Through Unconsolidated Sands," *Physics,* vol. 7, pp. 325-345, 1936/09 1936.
18. E. Lemmon, M. Huber, and M. McLinden, "NIST Standard Reference Database 23, Reference Fluid Thermodynamic and Transport Properties (REFPROP), version 9.0, National Institute of Standards and Technology," *R1234yf. fld file dated December,* vol. 22, 2010.
19. S. Berg, S. Oedai, D. van Batenburg, K. Elewaut, and D. Boersma, "Visualization of ASP Coreflood Experiments Using X-ray CT Imaging," in *IOR 2015-18th European Symposium on Improved Oil Recovery*, 2015.
20. D. D. Huang and M. M. Honarpour, "Capillary end effects in coreflood calculations," *Journal of Petroleum Science and Engineering,* vol. 19, pp. 103-117, 1998.